Aldehydes gas ozonation monitoring: Interest of SIFT/MS versus GC/FID

Leticia Vitola Pasetto, Valérie Simon, Romain Richard, Jean-Stéphane Pic, Frédéric Violleau, Marie-Hélène Manero

Accepted Manuscript

Aldehydes gas ozonation monitoring: Interest of SIFT/MS *versus* GC/FID

Leticia Vitola Pasetto, Valérie Simon, Romain Richard, Jean-Stéphane Pic, Frédéric Violleau, Marie-Hélène Manero

PII: S0045-6535(19)31427-4

DOI: https://doi.org/10.1016/j.chemosphere.2019.06.186

Reference: CHEM 24216

To appear in: *ECSN*

Received Date: 14 March 2019

Revised Date: 20 June 2019

Accepted Date: 24 June 2019

Please cite this article as: Vitola Pasetto, L., Simon, Valé., Richard, R., Pic, Jean.-Sté., Violleau, Fréé., Manero, Marie.-Héè., Aldehydes gas ozonation monitoring: Interest of SIFT/MS *versus* GC/FID, *Chemosphere* (2019), doi: https://doi.org/10.1016/j.chemosphere.2019.06.186.

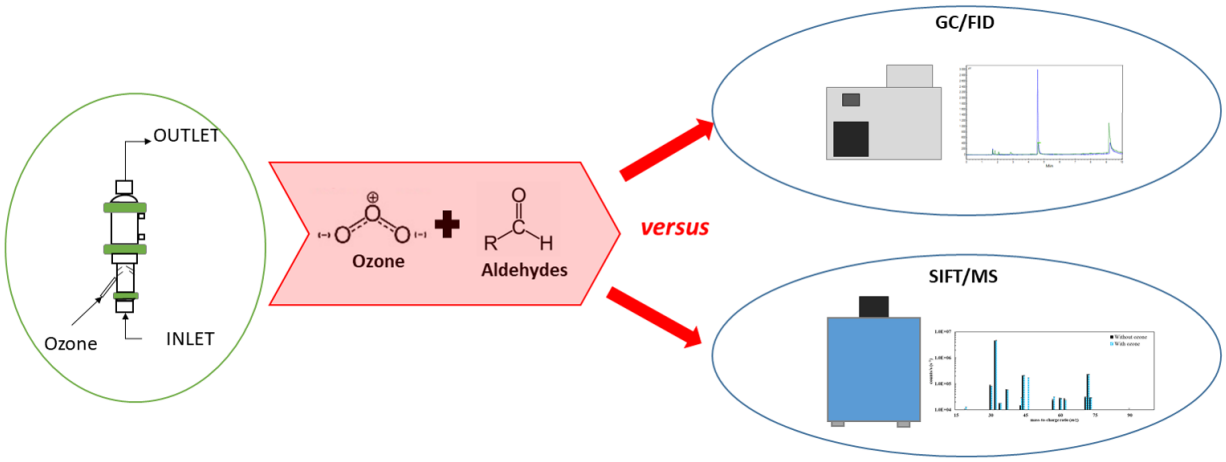

Comment citer ce document :
Vitola Pasetto, L., Simon, V., Richard, R., Pic, J.-S., Violleau, F., Manero (2019). Aldehydes gas ozonation monitoring: Interest of SIFT/MS versus GC/FID. Chemosphere. , DOI : 10.1016/j.chemosphere.2019.06.186

Aldehydes gas ozonation monitoring: interest of SIFT/MS *versus* GC/FID

Leticia Vitola Pasetto[1,2], Valérie Simon[2], Romain Richard[1], Jean-Stéphane Pic[3], Frédéric Violleau[2*], Marie-Hélène Manero[1]

(1) Laboratoire de Génie Chimique, Université de Toulouse, CNRS, INPT, UPS, Toulouse, France.
(2) Laboratoire de Chimie Agro-industrielle, LCA, Université de Toulouse, INRA, INPT-ENSIACET, Toulouse, France.
(3) Laboratoire d'Ingénierie des Systèmes Biologiques et des Procédés, Université de Toulouse, CNRS, INRA, INSA, Toulouse, France.

Abstract

Two analytical techniques – online gas chromatography coupled with flame ionization detector (often used method for VOCs monitoring) *versus* selected ion flow tube coupled with mass spectrometry (a more recent technique based on direct mass spectrometry) – were compared in association to an ozone-based gas treatment. Selecting aldehydes as the representative VOCs, their concentrations were monitored during ozonation experiments by both techniques in parallel. Contradictory results were obtained in the presence of ozone. Aldehydes were up to 90% removed due to a reaction with ozone according to GC/FID analysis, whereas with SIFT/MS, aldehydes concentration remained at the same level during the experiments regardless of the ozone presence. In addition, it was demonstrated that the apparent aldehydes removal was affected by GC injector temperature, varying from 90% (when it was at 250 °C) to 60% (at 100 °C). Meanwhile, even when the ozonation reactor was heated to 100 °C, no aldehydes conversion was evidenced by SIFT/MS, suggesting that the GC injector temperature was not the only interference-causing parameter. The ozone-aldehyde reaction is probably catalyzed by some material of GC injector and/or column. An ozone-GC interference was therefore confirmed, making unsuitable the use of GC/FID with silicone stationary phase to monitor aldehydes in presence of high concentrations of ozone (at least 50 ppmv). On the other hand, SIFT/MS was validated as a reliable technique, which can be employed in order to measure VOC concentrations in ozonation processes.

* Corresponding author. Email: frederic.violleau@purpan.fr . Tel. +33 5 61 15 29 78 Current address: Ecole d'Ingénieurs de PURPAN, 75 voie du TOEC, BP 57611, 31076 TOULOUSE Cedex 3, France

Keywords

ozone artifacts; aldehydes; GC/FID; SIFT/MS; gas treatment, VOC

Highlights

- Ozone interferes on aldehyde analysis by GC/FID with silicone-based column;
- Aldehyde-ozone reaction in GC system could lead to a process misinterpretation;
- SIFT/MS is a reliable technique to monitor VOCs in presence of ozone.

1. Introduction

Environmental chemistry field pays particular attention to volatile organic compounds (VOCs). Emitted from variety of sources, such as motor vehicles and chemical plants, these carbon-containing molecules play an important role in atmospheric photochemical reactions, in aerosol formation and some are harmful to human health (Parmar and Rao, 2009). In addition, some oxygenated volatile organic compounds (OVOCs) – such as aldehydes – are often associated to odor nuisance (Anet et al., 2013; Fang et al., 2012; Kolar and Kastner, 2010).

Among several treatments to reduce the environmental impact caused by VOCs, oxidation processes are of major concern. They are destructive processes, indicated for low pollutant concentrations and are often based on radical mechanisms. Plasma treatment, photocatalysis, catalytic oxidation and oxidative wet scrubbers are some examples of oxidation technologies (Martinez et al., 2014; Parmar and Rao, 2009; Thevenet et al., 2014; Vega et al., 2014). Thanks to its high oxidizing potential (Oyama, 2000), ozone (O_3) has been applied as oxidant in many VOCs abatement studies, such as: (*i*) ozonation of slurries (Bildsoe et al., 2012; Liu et al., 2011); (*ii*) chemical absorption/wet scrubber coupled with ozone as advanced oxidation process (Domeno et al., 2010; Kerc and Olmez, 2010; Vega et al., 2014) (*iii*) adsorption with or without regeneration (Brosillon et al., 2001; Monneyron et al., 2007); (*iv*) catalytic processes (Brodu et al., 2012; Kastner et al., 2008; Kolar and Kastner, 2010); (*v*) non-thermal plasma – which produces ozone as a by-product (Abou Saoud et al., 2018; Roland et al., 2005) and (*vi*) homogeneous gas ozonation (Zhang and Pagilla, 2013).

In order to correctly evaluate a VOCs abatement, the analytical technique must be carefully selected. It is even more a critical choice in case of complex systems, such as those in which ozone is present. VOCs monitoring/detection has mainly been carried out by gas chromatography (GC) (Aragón et al., 2000; Dewulf et al., 2002; Helmig, 1999; Woolfenden, 2010), including VOCs abatement studies that employ ozone (Abou Saoud et al., 2018; Bildsoe et al., 2012; Domeno et al., 2010; Huang et al., 2016; Kolar and Kastner, 2010; Li et al., 2018; Vega et al., 2014). Associating a chromatography column type with a GC detector – such as flame ionization (FID), sulfur chemiluminescence (SCD), mass spectrometry (MS), flame photometric (FPD) –, GC shows a high adaptability, making possible the detection of all classes of VOCs (sulfides, oxygenates, hydrocarbons, aromatics and nitriles) (Aragón et al., 2000; Dewulf et al., 2002). GC analysis can be carried out in two different sampling configurations: direct system, when the analytical system is connected online with the gas matrix by a sampling loop (Dewulf et al., 2002) or indirect system, by syringe/bag sampling or by a pre-concentration step based on thermally desorbable solid sorbents (Woolfenden, 2010). Besides the use as sampling method, the pre-concentration step, such as cryogenic trapping/cold trap and thermodesorption coupled with GC, have also been applied in order to analyze low pollutant concentrations or to lower detection limits (Pal and Kim, 2008; Tuduri et al., 2001; Woolfenden, 2010). Carbon or polymer-containing sorbent tubes – like GCB, Tenax GC, Tenax TA, Carbopack B, Carbopack X – and solid phase micro-extraction (SPME) with polydimethylsiloxane (PDMS), carbon molecular sieve (Carboxen), divinylbenzene (DVB) fibers are examples of pre-concentration techniques (Lee et al., 2006; Nicolas et al., 2007; Pal and Kim, 2008; Tuduri et al., 2001). In case of OVOC analysis – more specifically of carbonyl compounds, such as aldehydes and ketones –, derivatization techniques can also be used as an alternative. The most common derivatization agent is 2,4-dinitrophenylhydrazine (DNPH) cartridges. After reaction with carbonyl, DNPH generates hydrazones, which can be analyzed by high pressure liquid chromatography coupled with UV detector. Derivatization agent can also be impregnated on SPME fiber. For example, O-(2,3,4,5,6-pentafluorobenzyl)hydroxylamine hydrochloride (PFBHA) forms volatile oxime derivatives which can be analyzed by GC/MS (Bourdin and Desauziers, 2014; Szulejko and Kim, 2015; Zhu et al., 2015).

Nonetheless, ozone artifacts generation has been reported in literature when the use of sorbent tubes, SPME fibers or derivatization agents is associated to the presence of ozone in gas matrix (Kahnt et al., 2011; Lee et al., 2006; McClenny et al., 2001; Nicolas et al., 2007; Szulejko and Kim, 2015; Uchiyama et al., 2012). Ozone reacts with sorbent material (Tenax TA, Tenax GR, Carbopack B, GCB) – promoting its chemical decomposition – and/or reacts with the previously adsorbed analytes, causing substantial loss or even gain of VOC concentration (Lee et al., 2006; McClenny et al., 2001; Nicolas et al., 2007). In order to reduce the interference, a previous ozone removal step is indicated, applying scrubbers or denuders such as potassium iodide (KI) filters and 1,2-bis-(4-pyridyl) ethylene (BPE) cartridges. However, these materials can also adsorb VOCs, and so, preliminary tests are mandatory (Lee et al., 2006; Nicolas et al., 2007). The negative ozone interference due to artifacts generation on VOC monitoring by indirect GC system (using pre-concentration or sampling devices) has been well studied and highlighted in the literature. However, a potential ozone disturbance on VOC analysis by direct GC system has not been discussed, as far we know. Only one study (Klasson et al., 2003) has indicated an ozone reactivity with one specific type of GC column and a positive ozone interference on CO_2 analysis. This previous study has proposed to measure ozone – in an extremely high concentration range (1400 to 32600 ppmv of O_3) – by GC associated to thermal conductivity detector (TCD) through quantification of CO_2 generated from the reaction of ozone and the column coating (porous divinylbenzene homopolymer GS-Q column).

Techniques based on chemical ionization coupled with mass spectrometry (ICMS), such as proton transfer reaction (PTR/MS) and selected ion flow tube (SIFT/MS), have emerged as alternatives to GC methods. They are direct mass spectrometry techniques, in which no separation step is necessary, enabling instantaneous quantification of most volatile compounds (Majchrzak et al., 2018; Perraud et al., 2016; Smith and Spanel, 2005; Vitola Pasetto et al., 2019; Volckaert et al., 2016). Particularly, SIFT/MS is able to carry out real-time analysis, even in humid air samples, and can also separate isobaric compounds at wide concentration ranges (from pptv to ppmv), showing low detection limits and high sensitivity (Olivares et al., 2011; Smith and Spanel, 2005). As chemical ionization techniques are softer and therefore more selective processes (compared to electron impact usually applied in mass

spectrometry), SIFT/MS is used to analyze complex gas mixtures composed by several VOCs (Huffel et al., 2012; Noseda et al., 2010; Olivares et al., 2011; Prince et al., 2010). Moreover, SIFT/MS is also able to monitor inorganic compounds, such as ozone (Hera et al., 2017; Williams et al., 2002).

In this work, two analytical techniques – GC/FID and SIFT/MS – were compared in association to a gas ozonation process applied as an odor treatment. Considering aldehydes as VOCs representative odorous compounds, both analytical methods were installed in parallel at the outlet of an ozonation reactor to monitor aldehyde concentration in high ozone content (compared to ppbv level of standard tropospheric ozone concentration (Sicard et al., 2018)). In order to avoid a potential ozone interference caused by sorbent material or ozone scrubber, we have selected operating conditions in which pre-concentration step was not necessary, and thus, a direct GC sampling configuration was adopted.

2. Material and Methods

2.1. Chemicals

Propanal (PA) and butanal (BA) have been selected as the representative VOCs because they are common pollutants with low odor threshold limits (1 ppbv for PA (Nagata, 2003) and 0.5 ppbv for BA (Blazy et al., 2015)), often detected in gas emitted by odor sensitive sites (Anet et al., 2013; Kolar and Kastner, 2010). They were purchased from Sigma-Aldrich Inc. (USA), with ≥ 97% (PA) and ≥ 99% (BA) of purity.

Methanol, used as solvent for analytical calibration by liquid standard injection, was purchased from Panreac Química SLU (Spain) with ≥ 99.9% of purity.

2.2. Experimental Set-up

Figure 1 shows an overview of the experimental set-up that is composed of four sections: ozone generation; gaseous effluent generation; ozonation reactor and analytical methods.

In the ozone generation section, the ozone generator (HTU500 AZCO Industries Limited, Canada) was fed with dry air (dew point equal to -40 °C at 101.3 kPa), which gas flow was controlled by a mass flowmeter (SLA 5850S-B Brooks Instruments, USA).

In the gaseous effluent generation section, the aldehyde was injected and controlled *via* a syringe pump (PH 2000 Harvard Apparatus, USA) and using a 10 mL (SGE, Australia) or a

250 µL glass gastight syringe (Hamilton, USA). The aldehydes were vaporized by the dry air stream, which temperature and relative humidity were measured by a transmitter (HMT333, Vaisala, Finland) and gas flow controlled by a mass flowmeter (SLA 5850S-B Brooks Instruments, USA).

In order to study the reaction at higher temperatures (from 25 °C to 100 °C), a heated circulating oil bath (Model 1160S, VWR, USA) composed of a stainless steel smooth-coil immersed in a synthetic thermoliquid (Ultra 350, Lauda, Germany) bath was installed at the air stream before the vaporization system.

In the ozonation reactor section, the gas phase reaction was performed in a continuous flow, using a jacketed glass tubular reactor (250 mL). The reactor was kept at atmospheric pressure during all experiments (101.3 kPa) and heated using the synthetic thermoliquid from the heated circulating oil bath.

In the analytical methods section, ozone concentrations were measured by a UV analyzer (BMT 964, BMT MESSTECHNIK GMBH, Germany) directly after its production by the generator and by SIFT/MS (Voice 200*ultra*, Syft Technologies Ltd, New Zealand) after dilution at the ozonation reactor. The aldehydes were measured using GC/FID (Varian 3800, USA) and SIFT/MS, both analytical equipment being installed in parallel and directly to the reactor outlet in an online system.

All ozonation experiments were carried out in two steps: (*i*) stabilization step (only BA or PA and dry air were presented, *i.e.* with ozone generator off), during which the aldehyde concentration at the inlet of the reactor was measured (called $[aldehyde]_{without\ ozone}$) and (*ii*) ozonation step (under stable aldehydes-dry air matrix, the ozone generator was switched on and ozone was presented at the system), during which the aldehyde concentration at the outlet of the reactor was monitored (called $[aldehyde]_{with\ ozone}$).

2.3. Analytical Methods

2.3.1.GC/FID

The compounds were separated on a non-polar (5% phenyl) methylpolysiloxane Varian CP-SIL8 capillary column (30 m, 320 µm, 1µm), using helium as carrier gas at a flow rate of 2

mL min^{-1}. The 1000 µL sample loop was kept at 50 °C and 101.3 kPa. The injector temperature was initially set at 250 °C using a deactivated and inert liner with volume equal to 0.9 mL (5190-2293 model, Agilent Technologies, Inc., USA) and with a split flow ratio of 20:1 (leading to a residence time in the injector equals to 1.3 s). The oven temperature was kept at 40 °C for 6 min, ramped to 200 °C at 25 °C min^{-1} and held at 200 °C for 2 min, which resulted in a analysis time equals to 15 min. The FID detector temperature was maintained at 250 °C, with gas flows equal to 25 mL min^{-1} of He, 30 mL min^{-1} of H_2 and 300 mL min^{-1} of air.

2.3.2.SIFT/MS

In SIFT/MS, the analyte (neutral compound) can be chemically ionized by different precursor ions: three positive ions (H_3O^+, NO^+, O_2^+) and five negative ions (NO_2^-, NO_3^-, O_2^-, HO^-, O^-). These precursor ions were produced by microwave discharge and then selected by a first quadrupole mass filter so that only one precursor at a time was injected to the reaction chamber (flow tube) by a nitrogen flow (180 NmL min^{-1}) as carrier gas. The sample was introduced to the flow tube (kept at 115 °C and 0.07 kPa) by a calibrated capillary at 20 NmL min^{-1}. Even when several VOCs are present in sample gas, each compound reacts with a judiciously selected precursor ion and generates product ions with specific mass-to-charge ratios (*m/z*) that are quantified by a second quadrupole mass spectrometer (Michel et al., 2005; Smith and Spanel, 2005).

As in classical mass spectrometry devices, SIFT/MS operates in two modes: multiple ion monitoring (MIM) and full mass scans (FS). During FS mode – for each selected precursor ion – the second quadrupole spectrometer scans over a mass range covering from 15 to 250 *m/z*, calculating a count rate (signal intensity in s^{-1}) for each unit of *m/z*. Along with information about sample composition, a semi-quantitative analysis can also be obtained in FS mode if kinetic parameters are known. In MIM mode, only the precursor and characteristic product ions of the target compounds are monitored, following their count rates over a time interval (Olivares et al., 2011; Smith and Spanel, 2005).

In SIFT/MS, the analyte concentration is calculated by *Equation 1* based on the rate coefficient (k) of the reaction between the neutral compound and the precursor ion, the ratio between product ion count rate (P) and precursor ion count rate (I), and the reaction time in the flow tube (t) (Guimbaud et al., 2007; Smith and Spanel, 2005), which was set at 5 ms in the Syft model used for this project. During sampling, the analyte present in the sample ($[A]_{sample}$) is diluted by the carrier gas in the flow tube, whose analyte concentration ($[A]_{ft}$) depends on the operating conditions of the flow tube – temperature (T_{ft}), pressure (P_{ft}), sample flow (φ_s), carrier gas flow (φ_c) – and on the Boltzmann constant (k_b), as described by *Equation 2* (Smith and Spanel, 2005). At low analyte concentrations, *Equation 1* can be approximated to a linear correlation between $[A]_{ft}$ and P/I ratio (*Equation 3*), if the limit of $k[A]_{ft}t$ approaching zero is considered in the exponential expression (Smith and Spanel, 2005). This linear approximation is only valid when P/I is less than 0.4, *i.e*. the product ion count rate (P) does not represent more than 40% of its precursor count rate (I) and it only describes primary ionization reactions (without clusters formation). When more than one product ion is generated, P represents the sum of all product ion count rates (Smith and Spanel, 2005).

$$\frac{P}{I} = \frac{(1-e^{-k[A]_{ft}t})}{e^{-k[A]_{ft}t}} \quad (1)$$

$$[A]_{sample} = [A]_{ft} \frac{T_{ft} k_b}{P_{ft}} \frac{(\varphi_s + \varphi_c)}{\varphi_s} \quad (2)$$

$$\frac{P}{I} = k[A]_{ft}t \quad (3)$$

Based on the reactional mechanism proposed by Martinez (1982) and Voukides et al. (2009), carboxylic acids are potential by-products of aldehydes gas ozonation. Hence, butanoic acid was also monitored during the ozonation experiments along with BA and O_3. As shown in *Table 1,* Butanoic acid and BA are ionized by all positive precursor ions (H_3O^+, NO^+ and O_2^+) (Michalcikova and Spanel, 2014; Spanel et al., 2002, 1997; Spanel and Smith, 1998). Ozone is ionized by three negative precursor ions (NO_2^-, O_2^- and HO^-) (Williams et al., 2002) and

NO_2^- is the most indicated precursor ion for high concentrations (until 100 ppmv of ozone). In order to avoid overlapping of product ions, butanoic acid concentrations were quantified by NO^+ spectra and a product ion with a *m/z* ratio of 118, whereas butanal was monitored by product ions with *m/z* ratios equal to 44 and 72 in O_2^+ spectra. Ozone was determined with a *m/z* ratio of -62 in NO_2^- spectra.

2.3.3.Method performance

In GC/FID, the limit of detection (LOD) and quantification (LOQ) were calculated as three and ten times the background level, respectively, resulting in 0.02 ng for LOD and 0.07 ng for LOQ. In concentration units, LOQ obtained for BA was 0.5 ppmv. The gas calibration *via* syringe pump was performed with 5 levels of BA concentrations, between LOQ and 3200 times the LOQ, with a coefficient of determination (R^2) equal to 0.9962. The repeatability was of 15% for concentrations up to 100 times the LOQ and equal to 5% for the rest of the domain. The gas calibration was validated by direct injection of liquid standards using methanol as solvent. The difference between both calibration methodologies was of less than 6.5% for BA.

In SIFT/MS, the linearity is valid when the precursor ion is in excess compared to product ions. In order to verify the linearity range of SIFT/MS measurements for each selected precursor ion, a calibration procedure was carried out varying BA concentration from 0.15 ppmv to 15 ppmv and ozone from 1 ppmv to 100 ppmv, both in 4 levels. The coefficient of determination (R^2) of P/I ratio *versus* BA concentration at the flow tube was equal to 0.9852 (where P was the sum of product ions O_2^+ [44] and O_2^+ [72] and I was O_2^+ [32]), whereas for O_3 R^2 was equal to 0.9527 (considering P as NO_2^- [-62] and I as NO_2^- [-46]). From the linear regression of P/I ratio *versus* $[A]_{ft}$, it was also possible to obtain k, which was determined dividing the slope by the reaction time in the flow tube. For BA, k_{NO+} and k_{O2+} obtained by this procedure were equal to $(3.1 \pm 0.9) \times 10^{-9}$ cm^3 $molecule^{-1}$ s^{-1} and $(2.8 \pm 0.8) \times 10^{-9}$ cm^3 $molecule^{-1}$ s^{-1} respectively, which are similar to those reported by Spanel et al. (2002, 1997). In the case of ozone, k_{NO2-} was equal to $(1.7 \pm 0.4) \times 10^{-10}$ cm^3 $molecule^{-1}$ s^{-1}, which are also similar to previously reported values (Williams et al., 2002). In SIFT/MS, LOD was defined

as three times the standard deviation of the mean in the background measurements, which were calculated by blank spectra in absence of BA and O_3, according to the expression proposed by Milligan *et al*. (2007). LOD depends on the mean background count rate of the product ion at specific *m/z* ratio; on the time of measurement and on the sensitivity of SIFT/MS device (which represents how many product ions at the specific *m/z* ratio were produced for a given concentration of analyte) (Milligan et al., 2007; Ross, 2008). Considering 100 s of time analysis, the LOD for BA was 0.3 ppbv by O_2^+ [44] and O_2^+ [72] and 0.2 ppbv for NO^+ [71]. For ozone, LOD was equal to 40 ppbv by NO_2^- for 60 s of time analysis [-62].

In both analytical techniques, blank chromatograms and spectra were continuously obtained in order to verify the presence of pollutants in dry air and the absence of BA and O_3 in the system before the experiments. The parameters associated to analytical performance of PA are reported in the *Support Information*.

The uncertainties of ozone concentration measured by UV analyzer were calculated by the method of error propagation, considering the standard deviation of a measurement time of 15 min (data recorded each 30 s) and uncertainty of the analytical system (estimated at 25% for 100 ppmv of O_3 and < 1% for ozone concentration superior to 4000 ppmv). The uncertainties from the SIFT/MS quantification were obtained from LabSyft® Data Analysis and were equal to the standard deviation of the mean concentration for a measurement time of 300 s), whereas those from GC/FID were calculated by the standard deviation of at least three chromatograms.

3. Results and Discussion

3.1. Ozonation of aldehydes

Preliminary experiments were carried out to verify if SIFT/MS and GC/FID would result to similar removal efficiencies of aldehydes. Initially, ozonation of BA was conducted considering a reactor temperature ($T_{reactor}$) equal to 25 °C, relative humidity in the reactor (RH) at 0.1%, a residence time in the reactor (t_{RES}) of 2 s and ozone concentration at the reactor inlet equal to 69 ± 4 ppmv ($[O_3]_{in}$). These operating conditions were compatible with those applied by Kolar and

Kastner (2010), who have reported a removal efficiency of 80% through homogeneous reaction of aldehydes with ozone.

With a BA inlet concentration set point at 5 ppmv, *i.e.* when ozone was not fed into the reactor, concentrations measured by GC/FID and by SIFT/MS in absence of ozone ($[BA]_{without\ ozone}$) were respectively 5.5 ± 0.3 ppmv and 5.7 ± 0.1 ppmv, according to *Figure 2*. However, when ozone was sent into the reactor, BA concentration in presence of ozone ($[BA]_{with\ ozone}$) measured by GC/FID was 0.6 ± 0.1 ppmv, whereas by SIFT/MS was 5.3 ± 0.1 ppmv. GC/FID results suggest a removal efficiency of BA up to 90%, which did not tally with SIFT/MS measurements. Similar conflicting results were obtained for PA ozonation, as shown in *Figure SI-1* in *Support Information*.

3.2. Increasing of ozonation reactor temperature

Due to the contradictory results of outlet aldehyde concentrations obtained by GC/FID and SIFT/MS devices when $T_{reactor}$ was 25°C, complementary experiments were conducted only focusing on ozonation of BA, since the similarity of BA and PA behaviors have already been confirmed in the preliminary tests. By varying the $T_{reactor}$ from 25 °C to 100 °C, two aspects were simultaneously investigated: (*i*) the repeatability of conflicting results and (*ii*) the impact of reactor conditions on removal efficiency of BA, *i.e.* if ozone-aldehydes reaction (seen by GC/FID) really happens in the gas ozonation reactor.

BA concentrations were monitored by SIFT/MS and by GC/FID simultaneously and in the same operating conditions applied previously ($[BA]_{without\ ozone}$ set point at 5 ppmv, RH at 0.1% and t_{RES} equal to 2 s). As it is shown in *Figure 2*, in addition to 25 °C, 4 more levels of $T_{reactor}$ were investigated (45 °C; 65 °C; 85 °C and 100 °C) and with $[O_3]_{in}$ equal to 58 ± 6 ppmv in average. The ozonation of BA has shown to be independent of the reactor temperature, since BA concentration during ozonation step ($[BA]_{with\ ozone}$) stayed at a constant level even with temperature increase. In absence of ozone, GC/FID and SIFT/MS measured similar BA concentrations ($[BA]_{without\ ozone}$ equal to 4.6 ± 0.7 ppmv). However, when the reactor was fed by ozone, the

measurements were discordant whatever the temperature considered. According to GC/FID results, $[BA]_{with\ ozone}$ was 0.6 ± 0.2 ppmv for all reactor temperatures, while $[BA]_{with\ ozone}$ measured by SIFT/MS was 4.3 ± 0.6 ppmv. No variation between ozone concentration at the inlet ($[O_3]_{in}$) and outlet of the reactor ($[O_3]_{out}$) could be detected, due to its large excess (*Figure 2*).

In *Figure 3*, GC/FID and SIFT/MS analyses are compared at the extremes of $T_{reactor}$ range: 25 °C (*Figure 3*A and *Figure 3*B) and 100 °C (*Figure 3*C and *Figure 3*D). In presence of 58 ppmv of ozone, BA peak intensity (retention time of 4.6 min) in the GC chromatogram (*Figure 3*A and *Figure 3*C) decreased compared to the chromatogram profile without ozone, suggesting that around 85% of BA was removed from gas matrix through reaction with ozone. In addition to BA peak reducing, new chromatographic peaks also appeared in the chromatogram profile in presence of ozone for both reactor temperatures, which may indicate by-products generation. The biggest by-product peak (retention time of 9.2 min) was identified as butanoic acid by injection of liquid standards.

Regarding the SIFT/MS results, both characteristic product ions of BA at *m/z* 44 and 72 in O_2^+ spectra have shown the same count rate in presence or absence of ozone (*Figure 3*B and *Figure 3*D), which is also valid for precursor ion (O_2^+ [32]) and product ion of butanoic acid (O_2^+ [60] and O_2^+ [73]). From O_2^+ spectra, the ozone occurrence did not dramatically modify *m/z* and count rate distributions of BA-air matrix, except for *m/z* 46, which only appeared when ozone was present for both $T_{reactor}$. Peaks at *m/z* 46 and *m/z* 64 have also been detected in presence of ozone in H_3O^+ spectra (*Figure SI-2A* and *Figure SI-3A* in *Support Information)*, probably due to NO_2 production in the ozone generator, since NO_2^+ (*m/z* 46) is its characteristic product ion. The non-variability of *m/z* and count rate distribution, and consequently, of chemical composition in BA-air matrix was also confirmed by H_3O^+ spectra, NO^+ spectra and NO_2^- spectra for $T_{reactor}$ of 25°C and of 100°C (in *Figure SI-2* and *Figure SI-3* in *Support Information*, respectively).

Therefore, four aspects can be highlighted regarding the conflicting results: (*i*) the decrease of aldehyde concentrations and by-products generation according to GC/FID; (*ii*) the non-removal of aldehydes and no by-product generation based on SIFT/MS measurements; (*iii*) the repeatability

of GC/FID and SIFT/MS results in presence of ozone and (*iv*) the stable apparent removal of BA for $T_{reactor}$ varying from 25 °C to 100 °C. The association of these aspects suggests that the ozone-aldehydes reaction – previously assumed to be located in the reactor – occurs elsewhere between the GC inlet and the GC system.

3.3. Varying GC parameters

Some GC parameters were tested to verify a probable influence on aldehyde analysis, *i.e.* on the apparent aldehyde removal. As an aldehyde-ozone reaction seems to happen, the GC injection temperature ($T_{GC\ inj.}$) – set initially at 250 °C – showed the highest potential to be the interference-causing parameter. In addition, residence time in the injector was 1.3 s, based on the GC operating conditions (split ratio, column gas flow and liner volume).

The removal efficiency of BA was monitored when $T_{GC\ inj.}$ was varied from 250 °C to 100 °C, as shown in *Figure 4*. BA concentrations were measured by GC/FID with operating conditions kept constant ($[BA]_{without\ ozone}$ at 22 ppmv; $T_{reactor}$ at 25 °C; RH at 0.1% and $[O_3]_{in}$ at 163 ppmv). The attenuation of removal efficiency with decreasing of GC injector temperature suggests that GC operating conditions indeed affect the BA ozonation.

In the GC chromatograms in *Figure 5*A, the overlapped profiles for $T_{GC\ inj.}$ at 250 and 100 °C demonstrate that when ozone was not in the gas matrix, BA detection by GC/FID was not impacted by $T_{GC\ inj.}$ changing, which confirms that no thermal degradation of BA occurred due to high injector temperatures. However, in presence of ozone (63 ± 4 ppmv), the BA peaks in *Figure 5*B for $T_{GC\ inj}$ at 250 and 100 °C were no longer overlapped, but they were less intense than those without ozone. BA concentration decreased from 25 ± 2 ppmv to 4.2 ± 0.2 ppmv when $T_{GC\ inj}$ was set at 250 °C, whereas at $T_{GC\ inj}$ of 100 °C, the concentration decrease was smaller (from 25 ± 2 ppmv to 14 ± 1 ppmv).

The gain in BA concentration with $T_{GC\ inj}$ reduction only when ozone was added confirms that BA reacts with ozone somewhere in the GC system, and not in the reactor as it could be wrongly supposed if SIFT/MS analysis was not available.

Nonetheless, $T_{GC\ inj}$ may not be the only GC parameter that causes the interference on aldehydes analysis, since even when $T_{reactor}$ was at 100 °C, no removal efficiency was detected by SIFT/MS whereas it was observed by GC/FID at $T_{GC\ inj}$ equal to 100 °C.

Complementary experiments were conducted to better understand the role of the GC injector (detailed in *Figure SI-4* in *Support Information*). It was observed that the removal efficiency of BA measured by GC/FID mainly depended on ozone concentration, but it showed a light influence of the residence time in the GC injector.

Different models of inlet liner (model Topaz 23301, Restek Corporation, USA) and of GC capillary column (non-polar; 100% PDMS Rtx-1; 60 m, 320 µm, 1 µm) were tested using the same operating conditions ($T_{GC\ inj.}$ at 250 °C; split ratio equal to 20:1; $[BA]_{without\ ozone}$ at 30 ppmv; $[O_3]_{in}$ at 60 ppmv and RH equal to 0.1%), but similar removal efficiencies were achieved compared to the models described in *Analytical Methods*. In addition, BA removal did not change even when a longer capillary column was used, in which the dead time and the retention time of BA (9.15 min) were higher. It suggests that aldehyde-ozone reactions may not be affected by a longer analysis time, and consequently, the reaction does not happen during the passage of the gas through the capillary column. Furthermore – based on *Figure 3*, *Figure 5* and *Figure SI-1, Support Information* – the chromatographic peaks related to PA and BA were still present (at a smaller intensity) and narrow and symmetric peaks of the reaction product have appeared. According to Dettmer-Wilde and Engewald (2014), these chromatogram characteristics suggest that the aldehyde-ozone reactivity probably takes place in the injector or at column head, through a fast reaction that is completed before entering into the column.

Therefore, the ozonation of aldehydes in GC may occur due to a catalytic pathway. Some GC material could act as a catalyst, as it was already observed for metal oxides, zeolites and carbon-based materials which can enhance the ozone-oxidation of VOCs (Brodu et al., 2012; Kastner et al., 2008; Masuda et al., 2001; Oyama, 2000). On the surface of these catalysts, the ozone reacts with the active sites (Lewis acid site) to form secondary oxidizing agents (atomic oxygen, peroxide ions, hydroxyl radicals), which subsequently react with the pollutants (Abou Saoud et al., 2019; Brodu et al., 2018; Wang et al., 2018).

As far we know, the ozone decomposition on PDMS stationary phase has not been discussed in the literature. There are only studies that investigate the PDMS decomposition – in form of membranes or microfluidic systems – through reaction with ozone or in contact of non-thermal plasma (Alves dos Santos et al., 2015; Duffy et al., 1998; Fu et al., 2009). The aim of these studies was to explore the changing of material properties, which was not related to catalysis or degradation of VOC. Nevertheless, they have evidenced the reactivity between ozone and PDMS. Duffy *et al*, (1998), for example, have demonstrated that the attack of the non-thermal plasma was at the silicon atoms, converting the $–OSi(CH_3)_2O–$ groups on the surface to $–O_nSi(OH)_{4-n}O–$ groups. Another example is the studies conducted by Fu *et al* (2009) that have investigated the attack of ozone (generated by UV light) on membranes made by PDMS. Besides the generation of silanol groups (SiOH) on the polymeric chain – in accordance with Duffy *et al* (1998) – the authors have also identified the formation of an inorganic SiO_2 layer over the surface. In addition, the UV/ozone treatment has been applied to remove layer of organic compound present at the surface of PDMS membranes, due to generation of radicals and oxygen atom. Furthermore, these silanol groups exhibit acid properties, which could act as active sites and interact with polar analytes (Dettmer-Wilde and Engewald, 2014) and also decompose ozone, as demonstrated by Monneyron *et al*. (2003b) in their studies of catalytic ozonation using zeolites.

In summary, we could explain the conversion of aldehyde by a reaction of ozone with the silicone-based material of the GC column, which is enhanced by the high temperature of the GC injector and generates silanol groups. This silanol group could act as active sites and lead, in the presence of ozone, to the formation of radical species that react with the aldehydes.

4. Conclusion

An ozone-GC interference was evidenced in the operating conditions applied in this study (using silicone stationary phase), leading to falsely low aldehyde concentration in presence of ozone. Since GC injector temperature was not the only interference-causing parameter, the ozone-aldehyde reaction is probably catalyzed by some material of GC injector and/or column. In the case when GC/FID must

be applied to analyze an ozone-containing gas matrix, a preliminary ozone-removal step is thereby required.

The untrue aldehydes quantification by GC/FID could only be verified by comparison with a second analytical approach – SIFT/MS –, which is based on a different operation principle, and thereby, does not present the same drawbacks as GC. SIFT/MS is the most indicated analytical device to monitor VOCs in presence of ozone, since it has proven to yield reliable results and to be indifferent to ozone disturbance. In addition, SIFT/MS is a faster and more sensitive technique, which is an interesting advantage in the environmental odor context that often faces limitations related to low odor threshold limits.

The major outcome of this study is the warning of applying GC/FID for aldehyde detection in presence of ozone. The use of unsuitable analytical devices could lead to unreliable results, and if this analytical device is associated to chemical processes, it could result in a process misinterpretation. For example, in case of this study, due to the use of GC/FID using silicone stationary phase, aldehyde removal values could be wrongly attributed to gas ozonation treatment.

5. Acknowledgements

The authors gratefully acknowledge the financial support for the research by French National Agency for Research and Technology and Agro Innovation International (CIFRE 2015/1233). The authors thank Mr. Laurent Willain for his support and helpful advices.

6. References

Abou Saoud, W., Assadi, A.A., Guiza, M., Bouzaza, A., Aboussaoud, W., Soutrel, I., Ouederni, A., Wolbert, D., Rtimi, S., 2018. Abatement of ammonia and butyraldehyde under non-thermal plasma and photocatalysis: Oxidation processes for the removal of mixture pollutants at pilot scale. Chem. Eng. J. 344, 165–172. https://doi.org/10.1016/j.cej.2018.03.068

Abou Saoud, W., Assadi, A.A., Guiza, M., Loganathan, S., Bouzaza, A., Aboussaoud, W., Ouederni, A., Rtimi, S., Wolbert, D., 2019. Synergism between non-thermal plasma and photocatalysis: Implicationsin the post discharge of ozone at a pilot scale in a catalytic fixed-bed reactor. Appl.

Catal. B Environ. 241, 227–235. https://doi.org/10.1016/j.apcatb.2018.09.029

Alves dos Santos, F.R., Borges, C.P., da Fonseca, F.V., 2015. Polymeric materials for membrane contactor devices applied to water treatment by ozonation. Mater. Res. 18, 1015–1022. https://doi.org/10.1590/1516-1439.016715

Anet, B., Lemasle, M., Couriol, C., Lendormi, T., Amrane, A., Le Cloirec, P., Cogny, G., Fillières, R., 2013. Characterization of gaseous odorous emissions from a rendering plant by GC/MS and treatment by biofiltration. J. Environ. Manage. 128, 981–987. https://doi.org/10.1016/j.jenvman.2013.06.028

Aragón, P., Atienza, J., Climent, M.D., 2000. Analysis of organic compounds in air: A review. Crit. Rev. Anal. Chem. 30, 121–151. https://doi.org/10.1080/10408340091164207

Bildsoe, P., Adamsen, A.P.S., Feilberg, A., 2012. Effect of low-dose liquid ozonation on gaseous emissions from pig slurry. Biosyst. Eng. 113, 86–93. https://doi.org/10.1016/j.biosystemseng.2012.06.009

Blazy, V., de Guardia, A., Benoist, J.C., Daumoin, M., Guiziou, F., Lemasle, M., Wolbert, D., Barrington, S., 2015. Correlation of chemical composition and odor concentration for emissions from pig slaughterhouse sludge composting and storage. Chem. Eng. J. 276, 398–409. https://doi.org/10.1016/j.cej.2015.04.031

Bourdin, D., Desauziers, V., 2014. Development of SPME on-fiber derivatization for the sampling of formaldehyde and other carbonyl compounds in indoor air. Anal Bioanal Chem 406, 317–328. https://doi.org/10.1007/s00216-013-7460-6

Brodu, N., Manero, M.H., Andriantsiferana, C., Pic, J.S., Valdés, H., 2018. Gaseous ozone decomposition over high silica zeolitic frameworks. Can. J. Chem. Eng. 96, 1911–1918. https://doi.org/10.1002/cjce.23141

Brodu, N., Zaitan, H., Manero, M.H., Pic, J.S., 2012. Removal of volatile organic compounds by heterogeneous ozonation on microporous synthetic alumina silicate. Water Sci. Technol. 66,

2020–2026. https://doi.org/10.2166/wst.2012.385

Brosillon, S., Manero, M.-H.H., Foussard, J.-N.N., 2001. Mass transfer in VOC adsorption on zeolite: experimental and theoretical breakthrough curves. Environ. Sci. Technol. 35, 3571–3575. https://doi.org/10.1021/es010017x

Dettmer-Wilde, K., Engewald, W., 2014. Practical Gas Chromatography: A Comprehensive Reference. Springer. https://doi.org/10.1007/978-3-642-54640-2

Dewulf, J., Van Langenhove, H., Wittmann, G., 2002. Analysis of volatile organic compounds using gas chromatography. Trends Anal. Chem. 21, 637–646. https://doi.org/10.1016/S0165-9936(02)00804-X

Domeno, C., Rodríguez-Lafuente, A., Martos, J.M., Bilbao, R., Nerín, C., 2010. VOC removal and deodorization of effluent gases from an industrial plant by photo-oxidation, chemical oxidation, and ozonization. Environ. Sci. Technol. 44, 2585–2591. https://doi.org/10.1021/es902735g

Duffy, D.C., McDonald, J.C., Schueller, O.J.A., Whitesides, G.M., 1998. Rapid prototyping of microfluidic systems in poly(dimethylsiloxane). Anal. Chem. 70, 4974–4984. https://doi.org/10.1021/ac980656z

Fang, J.J., Yang, N., Cen, D.Y., Shao, L.M., He, P.J., 2012. Odor compounds from different sources of landfill: Characterization and source identification. Waste Manag. 32, 1401–1410. https://doi.org/10.1016/j.wasman.2012.02.013

Fu, Y.J., Qui, H.Z., Liao, K.S., Lue, S.J., Hu, C.C., Lee, K.R., Lai, J.Y., 2009. Effect of UV-Ozone treatment on poly(dimethylsiloxane) membranes: surface characterization and gas separation performance. Langmuir 26, 4392–4399. https://doi.org/10.1021/la903445x

Guimbaud, C., Catoire, V., Bergeat, A., Michel, E., Schoon, N., Amelynck, C., Labonnette, D., Poulet, G., 2007. Kinetics of the reactions of acetone and glyoxal with O_2^+ and NO^+ ions and application to the detection of oxygenated volatile organic compounds in the atmosphere by chemical ionization mass spectrometry. Int. J. Mass Spectrom. 263, 276–288.

https://doi.org/10.1016/j.ijms.2007.03.006

Helmig, D., 1999. Air analysis by gas chromatography. J. Chromatogr. A 843, 129–146.

Hera, D., Langford, V., McEwan, M., McKellar, T., Milligan, D., 2017. Negative reagent ions for real time detection using SIFT-MS. Environments 4, 16. https://doi.org/10.3390/environments4010016

Huang, Huiling, Huang, Haibao, Zhan, Y., Liu, G., Wang, X., Lu, H., Xiao, L., Feng, Q., Leung, D.Y.C., 2016. Environmental Efficient degradation of gaseous benzene by VUV photolysis combined with ozone-assisted catalytic oxidation : Performance and mechanism. "Applied Catal. B, Environ. 186, 62–68. https://doi.org/10.1016/j.apcatb.2015.12.055

Huffel, K. Van, Heynderickx, P.M., Dewulf, J., Langenhove, H. Van, 2012. Measurement of odorants in livestock buildings: SIFT-MS and TD-GC-MS. Chem. Eng. Trans. 30, 67–72.

Kahnt, A., Iinuma, Y., Böge, O., Mutzel, A., Herrmann, H., 2011. Denuder sampling techniques for the determination of gas-phase carbonyl compounds : A comparison and characterisation of in situ and ex situ derivatisation methods. J. Chromatogr. B 879, 1402–1411. https://doi.org/10.1016/j.jchromb.2011.02.028

Kastner, J.R., Ganagavaram, R., Kolar, P., Teja, A., Xu, C., 2008. Catalytic ozonation of propanal using wood fly ash and metal oxide nanoparticle impregnated carbon. Environ. Sci. Technol. https://doi.org/10.1021/es0707512

Kerc, A., Olmez, S.S., 2010. Ozonation of odorous air in wastewater treatment plants. Ozone Sci. Eng. 32, 199–203. https://doi.org/10.1080/01919511003792102

Klasson, K.T., Jones, S.A., Walker, A.B., 2003. Measurement of ozone via an indirect gas chromatography method. Ozone Sci. Eng. 25, 155–158. https://doi.org/10.1080/713610670

Kolar, P., Kastner, J.R., 2010. Low-temperature catalytic oxidation of aldehyde mixtures using wood fly ash: Kinetics, mechanism, and effect of ozone. Chemosphere 78, 1110–1115. https://doi.org/10.1016/j.chemosphere.2009.12.033

Lee, J.H., Batterman, S.A., Jia, C., Chernyak, S., 2006. Ozone artifacts and carbonyl measurements using Tenax GR, Tenax TA, Carbopack B, and Carbopack X adsorbents. J. Air Waste Manage. Assoc. 56, 1503–1517. https://doi.org/10.1080/10473289.2006.10464560

Li, Y., Cheng, S., Yuan, C., Lai, T., Hung, C., 2018. Removing volatile organic compounds in cooking fume by nano-sized TiO_2 photocatalytic reaction combined with ozone oxidation technique. Chemosphere 208, 808–817. https://doi.org/10.1016/j.chemosphere.2018.06.035

Liu, D., Feilberg, A., Adamsen, A.P.S., Jonassen, K.E.N., 2011. The effect of slurry treatment including ozonation on odorant reduction measured by in-situ PTR-MS. Atmos. Environ. 45, 3786–3793. https://doi.org/10.1016/j.atmosenv.2011.04.028

Majchrzak, T., Wojnowski, W., Lubinska-Szczygeł, M., Różańska, A., Namieśnik, J., Dymerski, T., 2018. PTR-MS and GC-MS as complementary techniques for analysis of volatiles: A tutorial review. Anal. Chim. Acta 1035, 1–13. https://doi.org/10.1016/j.aca.2018.06.056

Martinez, R.I., 1982. The mechanism of O_3-Aldehyde Reactions. Int. J. Chem. Kinet. 14, 237–249.

Martinez, T., Bertron, A., Escadeillas, G., Ringot, E., Simon, V., 2014. BTEX abatement by photocatalytic TiO_2-bearing coatings applied tocement mortars. Build. Environ. 71, 186–192. https://doi.org/10.1016/j.buildenv.2013.10.004

Masuda, J., Fukuyama, J., Fujii, S., 2001. Ozone injection into an activated carbon bed to remove hydrogen sulfide in the presence of concurrent substances. J. Air Waste Manag. Assoc. 51, 750–755. https://doi.org/10.1080/10473289.2001.10464310

McClenny, W.A., Colon, M., Oliver, K.D., 2001. Ozone reaction with n -aldehydes (n =4–10), benzaldehyde, ethanol, isopropanol, and n-propanol adsorbed on a dual-bed graphitized carbon–carbon molecular sieve adsorbent cartridge. J. Chromatogr. A 929, 89–100.

Michalcikova, R.B., Spanel, P., 2014. A selected ion flow tube study of the ion molecule association reactions of protonated (MH^+), nitrosonated (MNO^+) and dehydroxidated $(M-OH)^+$ carboxylic acids (M) with H_2O. Int. J. Mass Spectrom. 368, 15–22.

https://doi.org/10.1016/j.ijms.2014.04.010

Michel, E., Schoon, N., Amelynck, C., Guimbaud, C., Catoire, V., Arijs, E., 2005. A selected ion flow tube study of the reactions of H_3O^+ , NO^+ and O_2^+ with methyl vinyl ketone and some atmospherically important aldehydes. Int. J. Mass Spectrom. 244, 50–59. https://doi.org/10.1016/j.ijms.2005.04.005

Milligan, D.B., Francis, G.J., Prince, B.J., McEwan, M.J., 2007. Demonstration of selected ion flow tube MS detection in the parts per trillion range. Anal. Chem. 79, 2537–2540. https://doi.org/10.1021/ac0622678

Monneyron, P., Manero, M.H., Mathé, S., 2007. A combined selective adsorption and ozonation process for VOCs removal from air. Can. J. Chem. Eng. 85, 326–332. https://doi.org/10.1002/cjce.5450850307

Monneyron, P., Mathé, S., Manero, M.-H., Foussard, J.-N., 2003. Regeneration of high silica zeolites via Advanced Oxidation Processes-A preliminary study about adsorbent reactivity toward ozone. Chem. Eng. Res. Des. 81, 1193–1198. https://doi.org/https://doi.org/10.1205/026387603770866371

Nagata, Y., 2003. Measurement of odor threshold by Triangle Odor Bag method. Odor Meas. Rev. 118–127.

Nicolas, M., Ramalho, O., Maupetit, F.-O., 2007. Reactions between ozone and building products: Impact on primary and secondary emissions. Atmos. Environ. 41, 3129–3138. https://doi.org/10.1016/j.atmosenv.2006.06.062

Noseda, B., Ragaert, P., Pauwels, D., Anthierens, T., Van Langenhove, H., Dewulf, J., Devlieghere, F. rank, 2010. Validation of Selective Ion Flow Tube Mass Spectrometry for fast quantification of volatile bases produced on Atlantic Cod (Gadus morhua). J. Agric. Food Chem. 58, 5213–5219. https://doi.org/10.1021/jf904129j

Olivares, A., Dryahina, K., Navarro, J.L., Smith, D., Spanel, P., Flores, M., 2011. SPME-GC-MS

versus selected ion flow tube mass spectrometry (SIFT-MS) analyses for the study of volatile compound generation and oxidation status during dry fermented sausage processing. J. Agric. Food Chem. 59, 1931–1938. https://doi.org/10.1021/jf104281a

Oyama, S.T., 2000. Chemical and catalytic properties of ozone. Catal. Rev. 42, 279–322. https://doi.org/10.1081/CR-100100263

Pal, R., Kim, K., 2008. Gas chromatographic approach for the determination of carbonyl compounds in ambient air. Microchem. J. 90, 147–158. https://doi.org/10.1016/j.microc.2008.05.007

Parmar, G.R., Rao, N.N., 2009. Emerging control technologies for volatile organic compounds. Crit. Rev. Environ. Sci. Technol. 39, 41–78. https://doi.org/10.1080/10643380701413658

Perraud, V., Meinardi, S., Blake, D.R., Finlayson-Pitts, B.J., 2016. Challenges associated with the sampling and analysis of organosulfur compounds in air using real-time PTR-ToF-MS and offline GC-FID. Atmos. Meas. Tech. 9, 1325–1340. https://doi.org/10.5194/amt-9-1325-2016

Prince, B.J., Milligan, D.B., McEwan, M.J., 2010. Application of selected ion flow tube mass spectrometry to real-time atmospheric monitoring. Rapid Commun. Mass Spectrom 24, 1763–1769. https://doi.org/10.1002/rcm

Roland, U., Holzer, F., Kopinke, F.D., 2005. Combination of non-thermal plasma and heterogeneous catalysis for oxidation of volatile organic compounds: Part 2. Ozone decomposition and deactivation of γ-Al2O3. Appl. Catal. B Environ. 58, 217–226. https://doi.org/10.1016/j.apcatb.2004.11.024

Ross, B.M., 2008. Sub-parts per billion detection of trace volatile chemicals in human breath using Selected Ion Flow Tube Mass Spectrometry. BMC Res. Notes 1:41, 1–5. https://doi.org/10.1186/1756-0500-1-41

Sicard, P., Agathokleous, E., Araminiene, V., Carrari, E., Hoshika, Y., De Marco, A., Paoletti, E., 2018. Should we see urban trees as effective solutions to reduce increasing ozone levels in cities? Environ. Pollut. 243, 163–176. https://doi.org/10.1016/j.envpol.2018.08.049

578 Smith, D., Spanel, P., 2005. Selected Ion Flow Tube Mass Spectrometry (SIFT-MS) for on-line trace
579 gas analysis. Mass Spectrom. Rev. 24, 661–700. https://doi.org/10.1002/mas.20033

580 Spanel, P., Jib, Y., Smith, D., 1997. SIFT studies of the reactions of H_3O^+ , NO^+ and O_2^+ with a series
581 of aldehydes and ketones. Int. J. Mass Spectrom. Ion Process. 165/166 165/166, 25–37.

582 Spanel, P., Smith, D., 1998. SIFT studies of the reactions of H_3O^+ , NO^+ and O_2^+ with a series of
583 volatile carboxylic acids and esters. Int. J. Mass Spectrom. Ion Process. 172, 137–147.

584 Spanel, P., Van Doren, J.M., Smith, D., 2002. A selected ion flow tube study of the reactions of H_3O^+,
585 NO^+, and O_2^+ with saturated and unsaturated aldehydes and subsequent hydration of the product
586 ions. Int. J. Mass Spectrom. 213, 163–176.

587 Szulejko, J.E., Kim, K., 2015. Derivatization techniques for determination of carbonyls in air. Trends
588 Anal. Chem. 64, 29–41. https://doi.org/10.1016/j.trac.2014.08.010

589 Thevenet, F., Loganathan, S., Guaitella, O., Barakat, C., Rousseau, A., 2014. Plasma-catalyst coupling
590 for volatile organic compound removal and indoor air treatment : A review. J. Phys. D. Appl.
591 Phys. 47. https://doi.org/10.1088/0022-3727/47/22/224011

592 Tuduri, L., Desauziers, V., Fanlo, J.L., 2001. Potential of Solid-Phase Microextraction fibers for the
593 analysis of Volatile Organic Compounds in air. J. Chromatogr. Sci. 39, 521–529.

594 Uchiyama, S., Inaba, Y., Kunugita, N., 2012. Ozone removal in the collection of carbonyl compounds
595 in air. J. Chromatogr. A 1229, 293–297. https://doi.org/10.1016/j.chroma.2012.01.062

596 Vega, E., Martin, M.J., Gonzalez-Olmos, R., 2014. Integration of advanced oxidation processes at
597 mild conditions in wet scrubbers for odourous sulphur compounds treatment. Chemosphere 109,
598 113–119. https://doi.org/10.1016/j.chemosphere.2014.02.061

599 Vitola Pasetto, L., Richard, R., Pic, J.-S., Manero, M.-H., Violleau, F., Simon, V., 2019. Hydrogen
600 sulphide quantification by SIFT/MS: highlighting the influence of gas moisture. Int. J. Environ.
601 Anal. Chem. *In press*.

602 Volckaert, D., Heynderickx, P.M., Fathi, E., Langenhove, H. Van, 2016. SIFT-MS a novel tool for

603 monitoring and evaluating a biofilter performance. Chem. Eng. J. 304, 98–105.
604 https://doi.org/10.1016/j.cej.2016.04.138

605 Voukides, A.C., Konrad, K.M., Johnson, R.P., 2009. Competing mechanistic channels in the oxidation
606 of aldehydes by ozone. J. Org. Chem. 74, 2108–2113. https://doi.org/10.1021/jo8026593

607 Wang, X., Romanias, M., Thévenet, F., Rousseau, A., 2018. Geocatalytic uptake of ozone onto natural
608 mineral dust. Catalysts 8, 263. https://doi.org/10.3390/catal8070263

609 Williams, S., Campos, M.F., Midey, A.J., Arnold, S.T., Morris, R.A., Viggiano, A.A., 2002. Negative
610 ion chemistry of ozone in the gas phase. J. Phys. Chem. A 106, 997–1003.
611 https://doi.org/10.1021/jp012929r

612 Woolfenden, E., 2010. Sorbent-based sampling methods for volatile and semi-volatile organic
613 compounds in air Part 1: Sorbent-based air monitoring options. J. Chromatogr. A 1217, 2674–
614 2484. https://doi.org/10.15713/ins.mmj.3

615 Zhang, Y., Pagilla, K.R., 2013. Gas-phase ozone oxidation of hydrogen sulfide for odor treatment in
616 water reclamation plants. Ozone Sci. Eng. 35, 390–398.
617 https://doi.org/10.1080/01919512.2013.796861

618 Zhu, W., Koziel, J.A., Cai, L., Özsoy, H.D., Leeuwen, J.H. Van, 2015. Quantification of carbonyl
619 compounds generated from ozone-based food colorants decomposition using on-fiber
620 derivatization-SPME-GC-MS. Chromatography 2, 1–18.
621 https://doi.org/10.3390/chromatography2010001

Table and Figures

Table 1. Product ions of the reactions between BA, O_3 and butanoic acid with H_3O^+, NO^+, O_2^+ and NO_2^-, with their respective rate coefficients and branching ratios in SIFT/MS.

Precursor ion	Compound Molar mass (g/mol)	Butanal 72	Ozone 48	Butanoic acid 88
H_3O^+	k[a] Product ion [*m/z*] (BR[b])	3.8[c] $C_4H_9O^+$ [73] (95%)[c] $C_4H_7^+$ [55] (5%)[c]	-	2.9[d] $C_4H_9O_2^+$ [89] (91%)[d] $C_4H_7O^+$ [71] (9%)[d]
NO^+	k[a] Product ion [*m/z*] (BR[b])	3.1 $C_4H_7O^+$ [71] (100%)[c]	-	1.9[d] $NO^+.C_4H_8O_2$ [118] (77%)[d] $C_4H_7O^+$ [71] (23%)[d]
O_2^+	k[a] Product ion [*m/z*] (BR[b])	2.8 $C_2H_4O^+$ [44] (48%)[c] $C_4H_8O^+$ [72] (52%)[c]	-	2.1[d] $C_2H_4O_2^+$ [60] (78%)[d] $C_3H_5O_2^+$ [73] (17%)[d] $C_4H_8O_2^+$ [88] (5%)[d]
NO_2^-	k[a] Product ion [*m/z*] (BR[b])	-	0.17 NO_3^- [-62] (100%)	-

a. Rate coefficient given in units of 10^{-9} $cm^3molecule^{-1}s^{-1}$.
b. Branching ratio (BR) represents the product ion distribution (appearance percentage) when more than one precursor is generated.
c. Kinetic parameters from Spanel *et al.* (2002).
d. Kinetic parameters from Michalcíková and Spanel (2014).

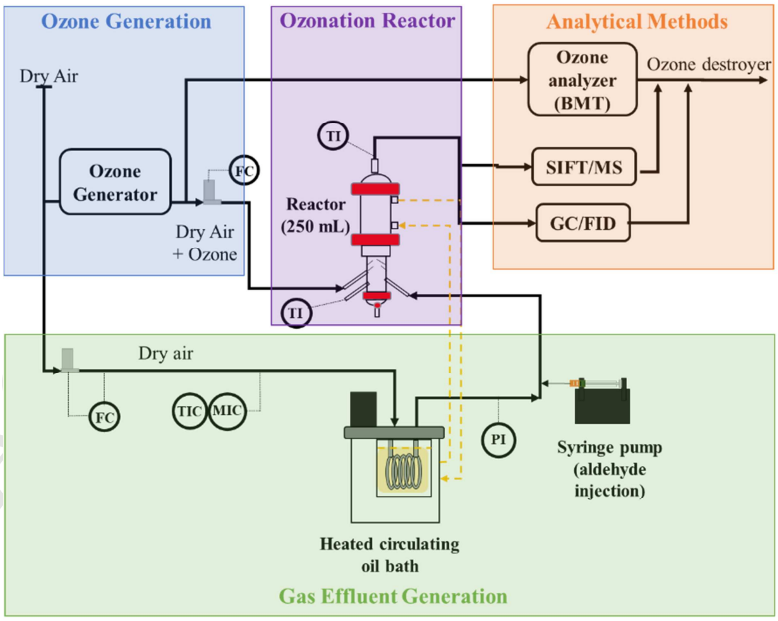

Figure 1. Experimental set-up.

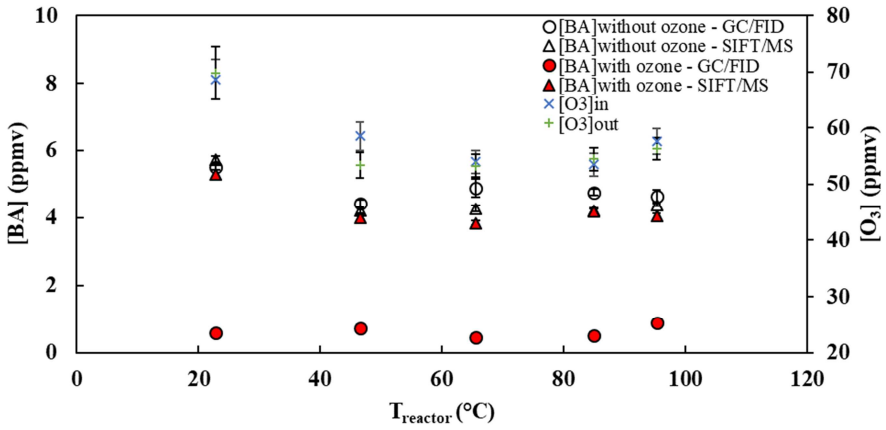

***Figure 2**. BA concentration measured by GC/FID and by SIFT/MS and ozone concentration measured by UV analyzer ($[O_3]_{in}$) and by SIFT/MS ($[O_3]_{out}$) for a range of reactor temperature with the same ozonation conditions: dry atmosphere (RH = 0.1%) and t_{RES} = 2 s.*

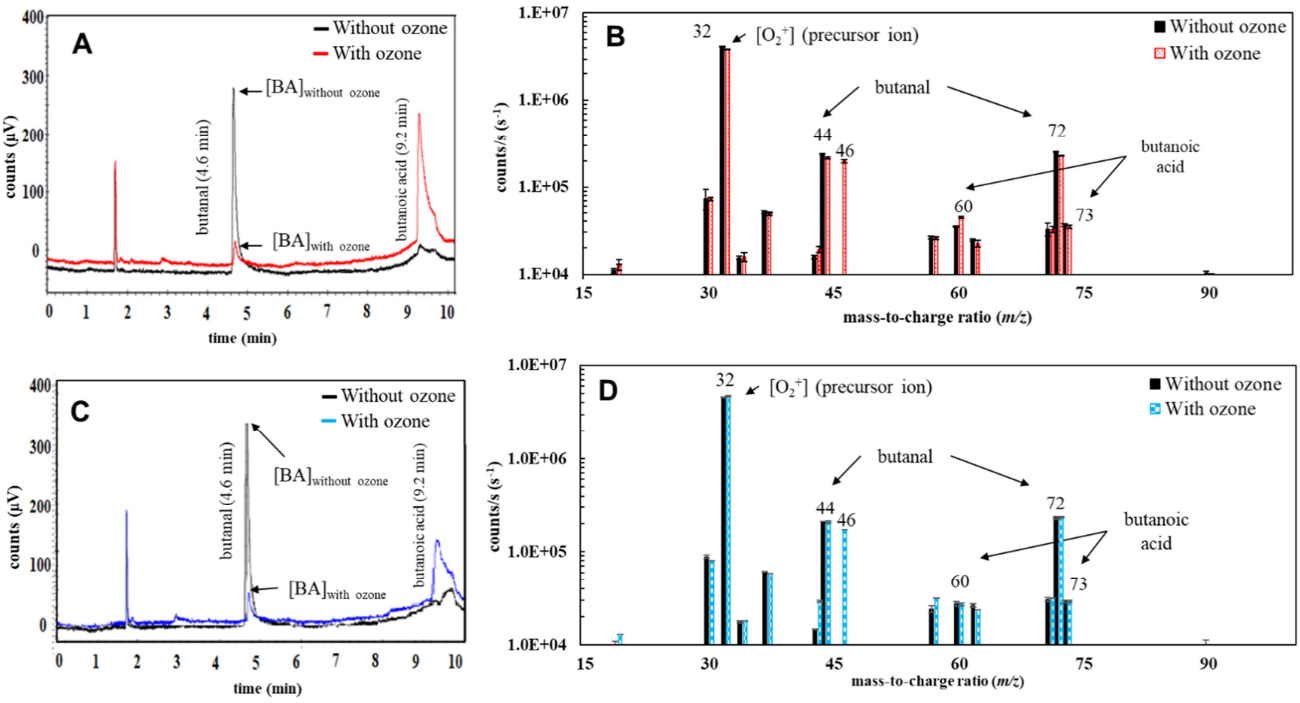

***Figure 3**. **A)** GC/FID chromatogram of BA detection in absence of ozone (black line) and in presence of ozone (red line) with $T_{reactor}$ = 25 °C. **B)** SIFT/MS full mass scan O_2^+ spectra of BA-air matrix without ozone (dark bars) and in presence of ozone (red dotted bars) with $T_{reactor}$ = 25 °C. **C)** GC/FID chromatogram of BA detection in absence of ozone (black line) and in presence of ozone (blue line) with $T_{reactor}$ = 100 °C. **D)** SIFT/MS full mass scan O_2^+ spectra of BA-air matrix without ozone (dark bars) and in presence of ozone (blue and striped bars) with $T_{reactor}$ = 100 °C.*

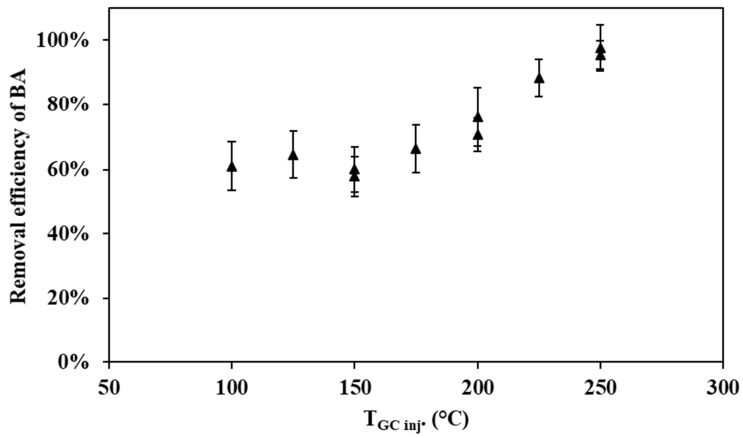

***Figure 4**. Removal efficiency of BA (▲) profile according to a range of $T_{GC\ inj.}$ under similar operating conditions in the reactor: $[BA]_{without\ ozone}$ = 22 ± 1 ppmv; $[O_3]_{in}$ = 163 ± 15 ppmv; dry atmosphere (RH = 0.1 %); $T_{reactor}$ at 25 °C and t_{RES} = 2 s.*

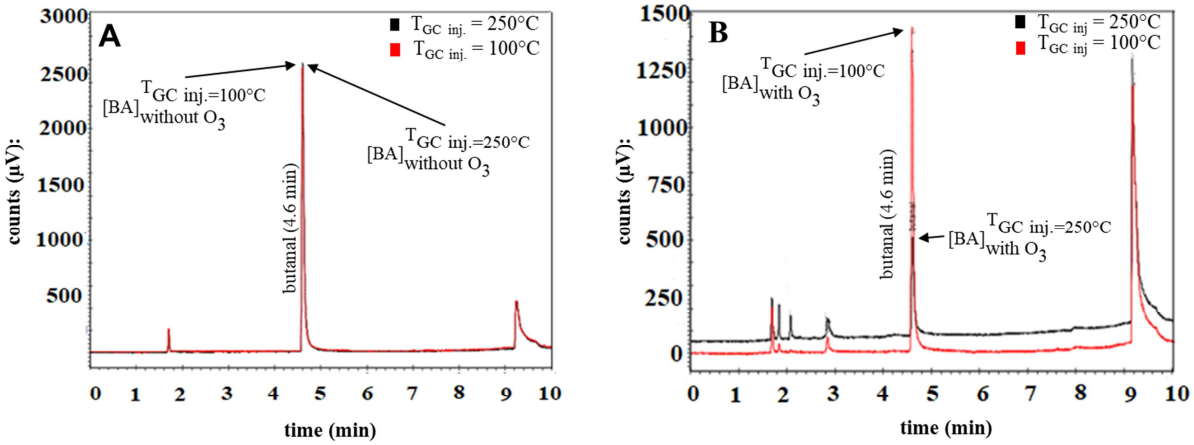

***Figure 5**. GC/FID chromatograms of BA detection carried out with $[BA]_{without\ ozone}$ at 25 ± 2 ppmv; $T_{reactor}$ at 25 °C; RH at 0.1% and $[O_3]_{in}$ at 63 ± 4 ppmv. **A**) Chromatogram profiles during stabilization time of BA-dry air matrix (without ozone) when $T_{GC\ inj.}$ was at 250 °C (dark line) and at 100 °C (red line). **B**) Chromatogram profile with ozone when $T_{GC\ inj.}$ was at 250 °C (dark line) and at 100 °C (red line).*